Correlation of changes in rheological properties with the growth kinetics of *Haematococcus pluvialis* in municipal wastewater

Uriel Carmona-Rosas [1], Roger Emmanuel Sales-Pérez [1], Joaquín Estrada-García [1], Eduardo Hernández-Aguilar [2] and Juan Manuel Méndez-Contreras [1,*]

[1] División de Estudios de Posgrado e Investigación, Tecnológico Nacional de México, Instituto Tecnológico de Orizaba, Orizaba, Veracruz, México
[2] Facultad de Ciencias Químicas, Universidad Veracruzana, Prol. De Ote. 6 número 1009, Colonia Rafael Alvarado. Orizaba, Veracruz. 94340. México
* Corresponding author: juan.mc@orizaba.tecnm.mx

Received: July 31, 2025 Accepted: September 3, 2025 Published: September 22, 2025
DOI: https://doi.org/10.56845/rebs.v7i2.566

Abstract: The objective of this research was to evaluate the biodegradation of municipal wastewater through the cultivation of *Haematococcus pluvialis* in a 4-L airlift photobioreactor over a period of 14 days, establishing the relationship between growth kinetics and changes in the rheological properties of the medium as a potential process monitoring strategy. To identify the ideal inoculum percentage, a unifactorial experimental design was implemented, where tests were conducted at different levels to determine statistically significant differences between them based on the biodegradation of organic matter. Three inoculum levels (5, 10, and 15%) were analyzed in 400 mL photobioreactors where cell growth, total COD, soluble COD, and pH were monitored. Once in the airlift photobioreactor, changes in shear stress and apparent viscosity were monitored in a range of 0.1–200 rpm, along with cell density growth and pollutant degradation (total COD, soluble COD, total nitrogen, and total phosphorus) every 2 days for 14 days. Laboratory-scale experiments showed soluble COD removals exceeding 95%, with the 15% inoculum level statistically showing the highest organic load removal. In the airlift reactor scale-up, a soluble COD removal percentage of 78% was achieved, and concentrations and concentrations values below the maximum permissible limits established by Mexican regulations (NOM-001-SEMARNAT-2021) were obtained for phosphorus and nitrogen content. The rheological monitoring showed an affinity to the Herschel–Bulkley model ($R^2 > 0.99$), with a decreasing trend observed in the consistency index (k), which decreased from 8.517×10^{-5} to 1.453×10^{-5}, and an increasing trend in the flow index(n), which rose from 1.583 to 1.905. This improvement is attributed to the reduction of soluble COD to values as low as 180 mg/L and to the increase in microalgal biomass, which reached up to 1.3×10^{7} cells/mL.

Keywords: Wastewater; *H. Pluvialis*; Rheological properties; Airlift reactor.

Introduction

In Mexico, the increasing generation of municipal wastewater constitutes a highly relevant environmental and public health problem. It is estimated that 76.8% (215.5 m^3/s) of the wastewater generated was collected in sewage systems, of which more than 40% does not receive adequate treatment before being discharged into receiving bodies of water (CONAGUA, 2022), which significantly contributes to the pollution of rivers, lakes, and aquifers. This situation is aggravated by the limited efficiency of conventional treatment technologies, which present technical and operational restrictions in the face of the increasing organic load and the presence of inorganic nutrients such as nitrogen and phosphorus that cause eutrophication of the environment. Furthermore, these systems usually require high energy demands because, in most cases, they require long periods of time to decompose complex organic compounds, which limits their effectiveness (Rout *et al*., 2021).

Another major problem is that these processes generate polluting byproducts; for example, activated sludge systems produce large volumes of residual sludge that require additional stabilization, dehydration, and final disposal processes (Wu *et al*., 2022), which pose environmental risks if not properly managed. On the other hand, conventional biological treatment generates greenhouse gases, mainly carbon dioxide (CO_2), nitrogen oxides (NO_x), and methane (CH_4) derived from the decomposition of organic matter. Taken together, these problems limit long-term sustainability and increase the need for new treatment alternatives (Singh *et al*., 2017).

Given this scenario, wastewater treatment with microalgae has emerged as a promising alternative in wastewater bioremediation processes due to its ability to assimilate organic and inorganic compounds, generate oxygen through photosynthesis, and produce value-added biomass. In particular, *Haematococcus pluvialis* is a green microalga of high biotechnological interest that has demonstrated a remarkable affinity for nutrients such as phosphorus and nitrogen, as well as efficient biomass accumulation under controlled cultivation conditions during its vegetative phase (Pan *et al*., 2021). This species is known for its production of extracellular polysaccharides (EPS), which can induce significant transformations in the rheological properties inside photobioreactors, in addition to promoting the aggregation and sedimentation of suspended and colloidal compounds (Laroche, 2022; Wang *et al*., 2019). While it has been shown that microalgae can grow in open environments, to obtain higher yields and better quality biomass, it is suggested that their propagation be carried out in isolated reactors. The airlift type is an ideal configuration to promote gentle but effective mixing without the need for moving parts; its hydraulic dynamics favor the homogenization of the culture, improving the transfer of gases such as CO_2 and O_2 (Uyar *et al*., 2024). Furthermore, it keeps the microalgal cells in suspension, reducing dead zones, preventing cell damage from shear stress, and improving the overall efficiency of the process. These particular conditions of controlled flow and continuous aeration can directly affect the rheological properties of the culture because as cell density increases and biomolecules such as EPS accumulate, the apparent viscosity of the medium can increase, altering the flow profile (Adesanya *et al*., 2012).

Previous studies have shown that microbial and algal growth in alternative biodegradation systems for wastewater and semi-solid waste can influence the rheological properties of culture media, suggesting their potential as indirect monitoring tools (Gutiérrez-Casiano *et al*., 2022; Estrada-García *et al*., 2023). However, the relationship between rheology and growth kinetics in *Haematococcus pluvialis* has not been thoroughly investigated, particularly under the complex conditions of municipal wastewater, which present both high organic load and compositional variability.

In this context, this study proposes the use of rheological characterization as a control and monitoring strategy for the treatment of municipal wastewater with H. pluvialis, linking rheological changes to cell growth dynamics and the reduction of organic load. It is proposed that changes in rheological properties, particularly in parameters such as the consistency index (k) and the flow index (n) of the Herschel-Bulkley model, may be correlated with increased cell density and the efficiency of removing dissolved organic matter (soluble and total COD). This approach not only allows for a better understanding of the system's physical-biological dynamics, but it can also represent a practical and non-invasive alternative for real-time operational decision-making.

Materials and Methods

Physicochemical and microbiological characterization of Municipal Wastewater (MWW)

Sampling was carried out using NMX-AA-003-1980 in a wastewater effluent within the flow of the "Rio Blanco" located in the municipality of Mendoza, Veracruz, Mexico, with a weekly frequency and during the season known as the winter drought in the period October-December. Physicochemical and microbiological characterization of municipal wastewater (MWW) was carried out to determine its composition and contaminant potential. Sampling was maintained until the physicochemical and microbiological parameters showed consistent values between consecutive samples, with standard deviations within narrow ranges. This criterion was considered indicative of a constant composition, ensuring a representative and characteristic profile of municipal wastewater during the winter dry season.

The characterization of the wastewater consisted of determining soluble COD (COD_s) and total COD (COD_T) using the method of standard NMX-AA-030/1_SCFI-2012; the content of total solids (TS) and total volatile solids (TVS), total nitrogen (TN) using the Kjeldahl method and total phosphorus (TP) were evaluated according to the Standard Methods for the Examination of Water and Wastewater 23rd Edition (2017) (APHA *et al*., 2017), and the determination of pH by the potentiometric method.

Experiments on the growth of H. Pluvialis

The microalga *H. pluvialis* was acquired from the company Algae Bank. Initially, the alga was propagated in M1B5 medium until a concentration of approximately 7.5 x 10^6 cells/mL was reached, sufficient to begin the adaptation and growth experiments in MWW (Radice *et al*., 2024). Figure 1 shows the experimental setup for the growth of *H. pluvialis* in MWW. To evaluate the efficiency of the bioremediation process, three inoculum levels (5%, 10%, and 15%) were established in 400 mL photobioreactors with three replicates for each (n=4).

Photobioreactors with different inoculum levels were maintained under constant aeration conditions of 1.2 L/min, constant temperature (20 ± 2 °C), and white light at 1000 lux in 12:12 (light:dark) photoperiods. All experiments were monitored every 3 days for a 14-day period, during which the following parameters were tracked: COD_T , COD_s , pH, and cell count. To identify the optimal inoculum percentage in the 400 mL photobioreactor trials, a unifactorial experimental design was implemented, in which tests were carried out at different levels to determine statistically significant differences among them based on the biodegradation of organic matter. Minitab 18.1 software was used for the statistical analysis.

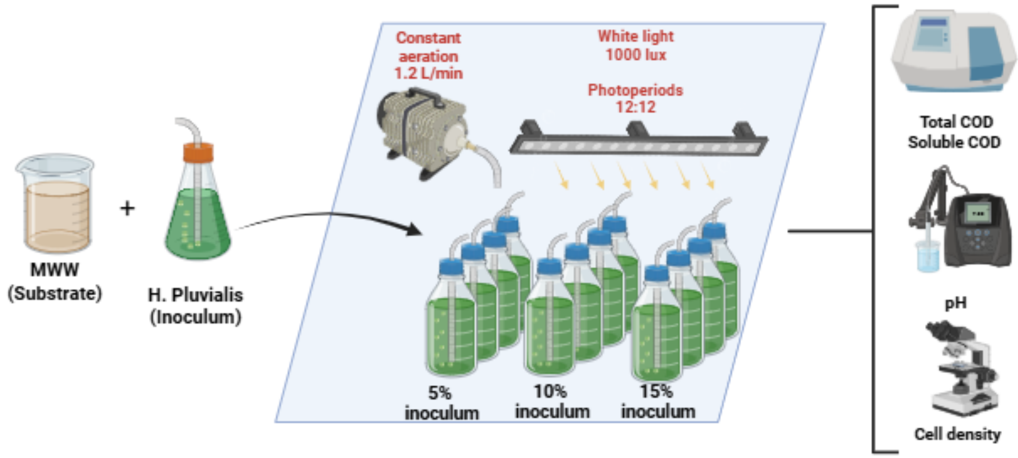

Figure 1. Bioconversion experiments using *H. Pluvialis.*

Cell density determination was performed using a Neubauer chamber, which has a central 1 mm² grid with 25 squares, each composed of 16 smaller squares. Its standard depth with the coverslip is 0.1 mm, taking into account the volume of the central quadrant: 1 mm² * 0.1 mm = 0.1 mm³ = 10^{-4} mL. Therefore, cell density was determined using Equation 1, taking into account that 25 squares were counted for greater accuracy, and the dilution factor was added as needed.

$$cell\ density\ \left[\frac{cells}{mL}\right] = \frac{number\ of\ cells * 250\ 000}{number\ of\ squares} = number\ of\ cells * 10\ 000 \quad \textbf{(1)}$$

Scaling up in airlift photobioreactors

The scaling up of experiments with *H. pluvialis* was carried out in a self-made airlift photobioreactor with a total volume of 5.5 L and a functional volume of 4 L. Figure 2 shows the design of the photobioreactor, where commonly used design parameters can be identified. It has been demonstrated that the correct proportion ratios favor efficient mixing, a homogeneous environment, and healthy cultivation without the need for mechanical agitation (Zhang *et al.*, 2014). The main column has a height of 68 cm (h_c). The main column has a height of 68 cm (h_c). The section where the gas and liquid are injected and rise is called the riser, which consists of an internal concentric tube with a diameter of 0.75 in (d_{dt}) and a height of 51 cm (h_{dt}). This tube, called the draft tube, was strategically placed 5 cm from the bottom of the photobioreactor (h_{bc}) to allow fluid recirculation. The gas sparger was located in this area and operated at a flow rate of 1.2 L/min.

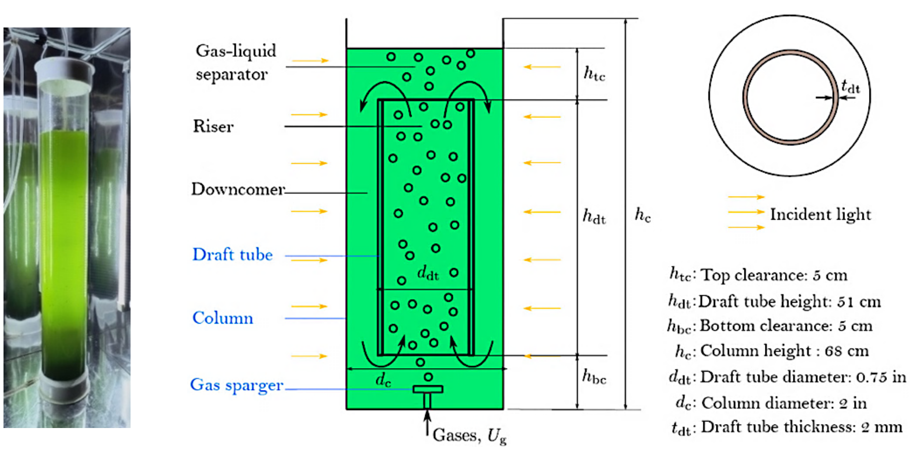

Figure 2. Design and photo of the photobioreactor used in the process. Adapted from (Li *et al.*, 2022)

At the top of the photobioreactor, a distance of 5 cm (h_{tc}) was established between the top of the inner concentric tube and the liquid level. In this area, the gas bubbles introduced to generate agitation and flow rise and are released, resulting in a physical separation between the liquid medium (microalgae) and the unabsorbed gas. For this reason, this area is called the gas-liquid separator zone (Behin & Amiri, 2023). In the part where there is no gas flow, the liquid descends by gravity due to the density difference with the ascending zone; this zone is called the downcomer zone (Mazziero *et al*., 2022).

To determine the inoculum percentage for scale-up in the airlift photobioreactor, the selected criterion was the ability to achieve the maximum permissible limits of soluble COD (sCOD) removal in the shortest possible time within the evaluated period (14 days), while simultaneously avoiding potential inhibition derived from excessive inoculum loads. The light, ventilation, and temperature conditions remained the same as in the previous phase. Samples were taken every 48 hours for 14 days to analyze the behavior of COD_T, COD_S, TN , TP, cell count, and rheological variables.

Rheological variable monitoring was performed using a Brookfield DV2T rotational viscometer with the ULA spindle. Viscosity (cP), torque (%), shear stress (Pa), and shear rate (s^{-1}) values were recorded at different angular velocities, initially in 1 rpm intervals up to 10 rpm, and subsequently from 10 rpm to 200 rpm. Shear stress was plotted against shear rate to generate rheograms; these results were then fitted to the Herschel-Bulkley, Ostwald-de Waele, and Newtonian rheological models (Equations 2-4). From these equations, rheological parameters were obtained, such as the consistency index (k), the flow index (n), the yield stress (τ_0), and the apparent viscosity (Pa·s).

$$\tau = k \cdot \dot{\gamma}^{n} \quad \textbf{(2)}$$

$$\tau = \tau_0 + (k \cdot \dot{\gamma}^{n}) \quad \textbf{(3)}$$

$$\tau = \eta \cdot \dot{y} \quad \textbf{(4)}$$

Results and Discussion

The results of the physicochemical characterization of the municipal wastewater are shown in Table 1. It should be noted that the pH can be considered neutral; this is due to several factors such as the presence of organic acids and bases in the municipal wastewater, fostered by microbiological activity with aerobic and anaerobic bacteria which produce carbonic acid and ammonia, causing a natural equilibrium tending to self-regulate the medium at a neutral pH (Huang *et al*., 2021). The pH value obtained in this study is within the range reported by Pérez-Guzmán *et al*. (2024), who mention that for municipal effluents the pH reached a value of 8.19; this parameter in both cases remained within the permissible range according to Mexican regulations (NOM-001-SEMARNAT-2021).

Table 1. Physicochemical characterization of municipal wastewater.

Parameter	Units	Average value MWW	Standard deviation
pH	-	7.90	±0.23
TS	mg/L	2066	±160
VTS	mg/L	1701	±145
COD	mg/L	2592	±324
Soluble COD	mg/L	785	±123
TP	mg/L	17	±2
TN	mg/L	32	±4

The wastewater showed high values of COD_T and COD_S (2595 mg/L and 785 mg/L respectively), which is attributed to the dry season during which the samples were taken. Both values were above the maximum permissible limit, as were the total suspended solids, indicating a high organic load. The values obtained are similar to those reported by Ata *et al*. (2021), where average COD values of 2367 mg/L were reached in the June–November period and the sampling points were located at the inlet of untreated water from different treatment plants.

A TN concentration of 32 mg/L was obtained, which is within the range of 30-35 mg/L reported in the literature for municipal wastewater (Tang *et al.*, 2023). The amount of TN is directly related to the urea content in human urine, which is a typical component in the composition of this effluent and increases the nitrogen present, mostly in the form of ammonium (Simha *et al.*, 2023). The TP content found was 17 mg/L, higher than that reported in the literature (Han *et al.*, 2021) in the range of 4.3-5.5 mg/L. This is attributable to the high content of detergents and cleaning products, which contribute synthetic phosphates (Azam & Finneran, 2013). Nitrogen and phosphorus are considered pollutants that promote the eutrophication of water bodies, causing an imbalance in the ecosystem; however, in bioremediation systems using microalgae, these nutrients are consumed and tend to be the main precursors of cell growth and development (De Moraes *et al.*, 2023).

Figure 3a shows the growth assays of *H. pluvialis* in MWW, where a similar cell density is observed at the beginning of the experiments in the 3 inoculum levels; however, statistically significant differences were found, indicating that a higher cell density was achieved with the 5% inoculum. The exponential growth phase was found to begin on day 10, where a deceleration in the increase of cell density is observed with the highest inocula (10% and 15%). The tendency of the lower inocula to reach higher cell concentrations is recurrent in wastewater bioremediation systems, as mentioned by Sales-Pérez *et al*. (2023b), where they used *N. oculata* for the treatment of poultry wastewater, varying the amount of inoculum at 3 levels (10%, 15%, and 20%), obtaining higher cell densities with the lower inoculum, while the higher inocula showed inhibition. This is generally attributed to the fact that in inocula with high volumes, nutrients (P, N, and C) are consumed quickly and with greater competition (Khalid *et al.*, 2018). Another factor to consider is that in systems with high cell density, light access to the culture is reduced, mainly in the area of the photobioreactor walls, producing a self-shading effect inside, generating inefficient nutrient consumption and producing growth inhibition (Jeong & Jang, 2021).

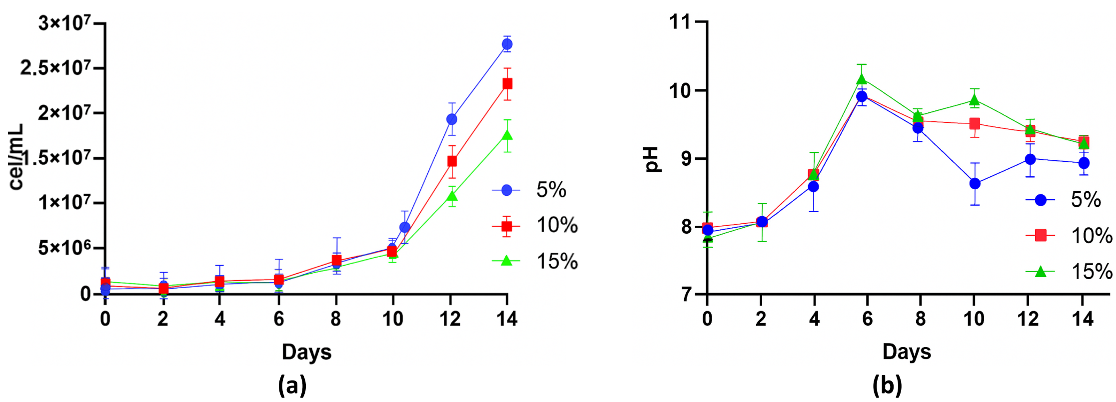

Figure 3. (a) Cell growth kinetics of *H. pluvialis* in MWW, (b) pH values determined during the growth of *H. pluvialis*.

Microalgae exhibit their highest growth rate in culture media with a pH between 7.0 and 8.4, a range in which bicarbonate (HCO_3^-) constitutes the predominant form of available inorganic carbon (Onyeaka *et al.*, 2021). Figure 3b shows the variations in pH values during the experiment with the 3 inoculum levels. Similar behavior was found for all three inoculum levels, where from day 2 onwards there was an increase in pH until day 6. From that day until the end of the experiment, fluctuations between 10 and 8.5 were recorded. This tendency to alkalinize the medium is characteristic of microalgae systems and is directly related to the assimilation of carbon present in the wastewater by the microalgae. During the photosynthesis process within photobioreactors, microalgae rapidly fix CO2 in a reaction that initiates the Calvin-Benson cycle, ultimately producing carbohydrates (Amaro *et al.*, 2023). This CO2 removal reaction shifts the carbonate system equilibrium, favoring the dissociation of bicarbonate (HCO_3^-) and carbonate (CO_3^{2-}), which generates hydroxyl ions and causes alkalinization of the medium, as shown in equations 5 and 6 (Abdel-Raouf *et al.*, 2012).

$$2(HCO_3^-) \rightarrow CO_3^{2-} + H_2O + CO_2 \qquad \textbf{(5)}$$

$$CO_3^{2-} + H_2O_2 \rightarrow 2OH^- + CO_2 \qquad \textbf{(6)}$$

Microalgae treatments promoted the biodegradation of organic pollutants, converting them into simpler molecules and using the assimilated carbon for their growth and development (Zhou *et al*., 2022). Figure 4a shows the COD removals during the experiments with the 3 inoculum levels, which removed concentrations between 64-74% of COD, similar to those reported by Abdel-Raouf *et al*. (2012) who obtained 67% COD removals for biological systems in wastewater treatment using microalgae. In the removal of total COD, it is common to find a point in these types of systems where it no longer decreases; this may be due to a combination of several factors, such as the cell lysis process due to the stress caused by the aeration system, which causes the release of intracellular content, compensating for the preliminary COD reduction (Qiu *et al*., 2017). Furthermore, it should be mentioned that in the stationary phase of cell growth, an equilibrium is reached between the COD removal rate and the biomass generation rate (Sobolewska *et al*., 2024), which is organic matter susceptible to degradation, which may explain why no considerable COD reduction occurred after day 8. Regarding the statistical analysis, no significant differences were observed in tCOD removal among the three inoculum levels evaluated (one-way ANOVA, $p > 0.05$, $n = 4$). Post-hoc comparisons (Tukey's test) confirmed the absence of statistically significant pairwise differences. This lack of significant differences may be explained by the fact that tCOD includes both soluble and particulate organic fractions; while inoculum size can enhance the biodegradation of soluble organic matter, the particulate fraction tends to be less biodegradable and largely unaffected by inoculum concentration. Consequently, variations in inoculum percentage exerted only a minor influence on overall tCOD removal efficiency.

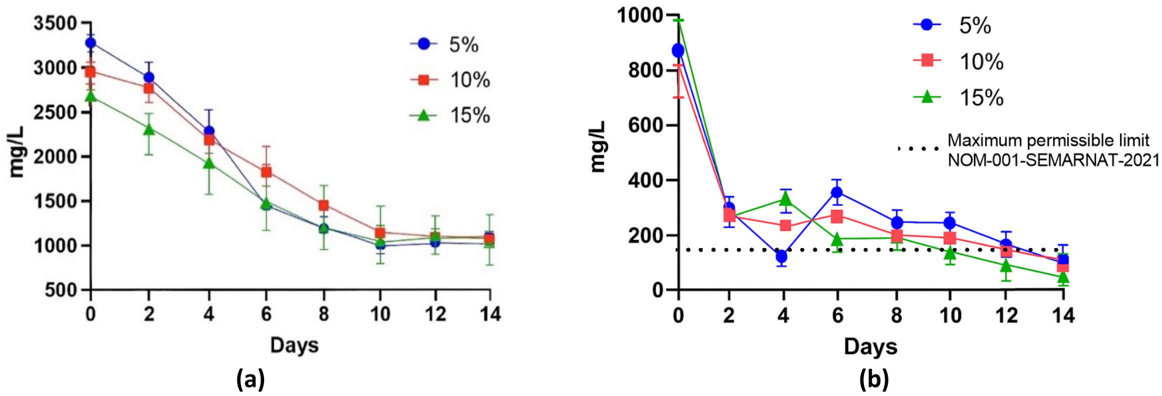

Figure 4. Behavior of the removal of (a) COD_T (b) COD_S.

Soluble COD (COD_s) is mainly composed of dissolved organic compounds and low molecular weight colloidal material (Płuciennik-Koropczuk & Myszograj, 2019). Figure 4b shows the removal of COD_S with the different inoculum concentrations evaluated, where a decreasing trend was observed from day 2 onwards, with removals of up to 70% for all experiments. Between days 2 and 10, fluctuating behavior was observed, with no significant changes in COD levels. Finally, after day 12, in all cases a decrease is observed until levels below the maximum permissible levels established in NOM-001-SEMARNAT-2021 (dotted line) are reached, obtaining a total removal of 92% - 99% for the 3 inoculum levels. However, statistically significant differences ($p < 0.05$, one-way ANOVA, $n = 4$) were observed among the inoculum percentages evaluated. Post-hoc analysis (Tukey's test) revealed that the highest COD_s removal percentages were obtained with 15%, which is consistent with the findings of Gentili (2014) who obtained a 92.7% removal of COD_s using Scenedesmus sp. in municipal wastewater combined with industrial wastewater. The decrease in COD in microalgae systems is caused by various factors, one of the main ones being the generation of EPS during microalgae metabolism. These compounds promote coagulation and the formation of flocs of colloidal particles; this new solid fraction is removed using mechanical operations such as centrifugation or sedimentation, thus reducing the COD concentration in the liquid phase (Xu *et al*., 2023).

Among the tested conditions, the 5% inoculum promoted the highest cell concentration, whereas the 15% inoculum achieved the greatest sCOD removal. However, only the 10% inoculum simultaneously ensured compliance with the regulatory discharge limits within the experimental timeframe in the shortest period, without exceeding biomass levels that could compromise reactor stability. Based on this predefined criterion, the 10% inoculum was selected for the scale-up experiments.

Figure 5a shows the results obtained in the airlift photobioreactor with *H. pluvialis* for the bioremediation of municipal wastewater; the green line shows cell growth and the blue line shows the decrease in COD_S over 14 days. The cell growth curve shows that the 0-6 day period was an adaptation phase; after that, a maximum concentration of 1.3 x 10^7 cells/mL was reached. Robles-Heredia *et al.* (2016) reported a similar maximum growth of 1.18 x 10^7 cells/mL of *Chlorella vulgaris* in an 11 L airlift photobioreactor. However, in this case, a lower cell concentration was obtained compared to experiments with 400 mL photobioreactors. This result is a common phenomenon when scaling up biological systems and can be explained by several interrelated factors affecting the availability of light, gases, and nutrients (Benner *et al.*, 2022; Xu *et al.*, 2009).

Figure 5a shows the behavior of COD_S during the 14 days of experimentation in the bioremediation system with the airlift-type photobioreactor. A significant decrease in COD_s was observed from day 2 until reaching values close to the maximum permissible limits from day 12, and by day 14 a maximum removal of 80% was achieved. This reduction can be explained by a series of synergistic mechanisms of a biological and physicochemical nature that operate simultaneously during the process. Firstly, during microalgal photosynthesis, CO_2 is used for biomass generation and the production of molecular oxygen (O_2). The O_2 acts as a terminal electron acceptor for heterotrophic bacteria that degrade dissolved organic compounds of low molecular weight such as volatile fatty acids, simple carbohydrates, and hydrosoluble proteins (Mathew *et al.*, 2022). This is complemented by the secretion of EPS, which, as already mentioned, act as natural flocculants that also promote the coagulation of colloidal particles, that is, they transform the COD_S into a particulate fraction that is easily removed by sedimentation or filtration.

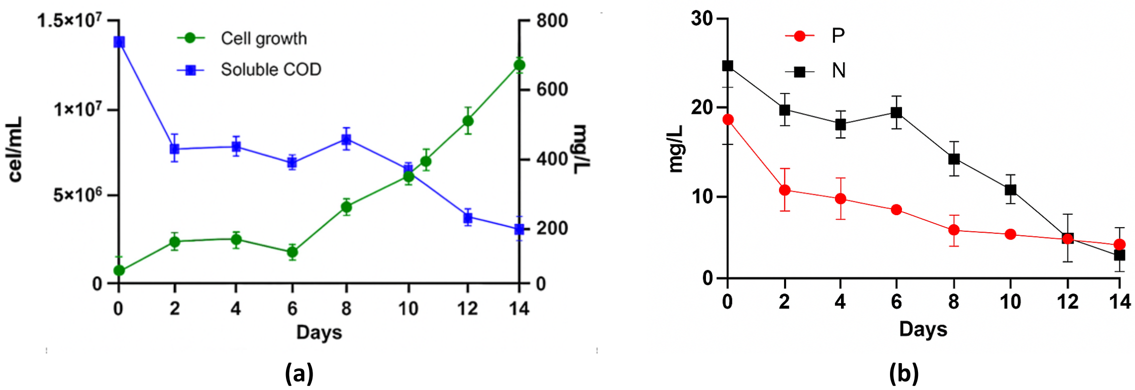

Figure 5. Behavior of the bioremediation process using *H. pluvialis* within the airlift FBR: (a) Removal of COD_S and cell growth; (b) Consumption of TP and TN.

The reduction of TP and TN in bioremediation systems represents a key component for the efficient treatment of wastewater, especially given the need to comply with environmental regulations in order to counteract eutrophication (Whitton *et al.*, 2015). Figure 5b shows the decrease in concentration of TP (black line) and TN (red line), where removal percentages of 77% and 89% were obtained, respectively, both complying with the maximum permissible limits established by Mexican regulations (NOM-001-SEMARNAT-2021). It should be noted that this process was carried out under conditions characteristic of maintaining the vegetative phase of *H. pluvialis*, which favored the assimilation and consumption of these nutrients because, in this physiological phase, it has a high demand for nutrients to sustain the synthesis of essential biomolecules (Nahidian *et al.*, 2018). In this study, the greatest reduction in phosphorus and nitrogen was observed during the active growth phase (between days 10-14), indicating that removal was mainly dominated by biological processes. Firstly, the nitrogen presents in the municipal wastewater in the form of ammonium (NH_4^+), nitrate (NO_3^-), and other organic forms, was incorporated by the microalgae for the synthesis of amino acids, proteins, nucleic acids, and pigments (Vega, 2018). On the other hand, phosphorus is absorbed as orthophosphate (PO_4^{3-}) and used in the formation of ATP, membrane phospholipids, and nucleic acids through phosphorylation (Su, 2020).

It has been demonstrated that the design of the photobioreactor directly influences the efficiency of bioremediation systems that use microalgae for wastewater treatment (Fu *et al.*, 2019). The proposed design configuration and parameters allowed for continuous and smooth mixing, which prevented the presence of dead zones and cell shearing, and also promoted homogeneous distribution of light and nutrients. This increased the efficiency of the cultivation and reaction conditions, allowing the processes of organic matter degradation, cell growth, and nutrient consumption to develop more efficiently, especially compared to static or poorly aerated systems.

In wastewater bioremediation systems that use microalgae, the incorporation of monitoring and control tools is fundamental to increasing process efficiency. In this context, rheology emerges as a valuable tool for evaluating the real-time state of the microalgal culture and its influence on the operation of the photobioreactor. This perspective is especially relevant in airlift-type photobioreactors, where the movement of the culture depends exclusively on the flow dynamics induced by aeration. Figure 6a shows the flow curves of the initial and final samples extracted from the photobioreactor during the bioremediation process. An increase in shear stress is observed in the final sample (blue line) compared to the initial sample due to the increase in biomass concentration during the photobioreactor's operation period. As the microalgae grew, a denser and more structured medium was generated. This higher cell concentration implies a greater resistance to flow, which translates into a higher shear stress, shifting from near-Newtonian to non-Newtonian behaviors.

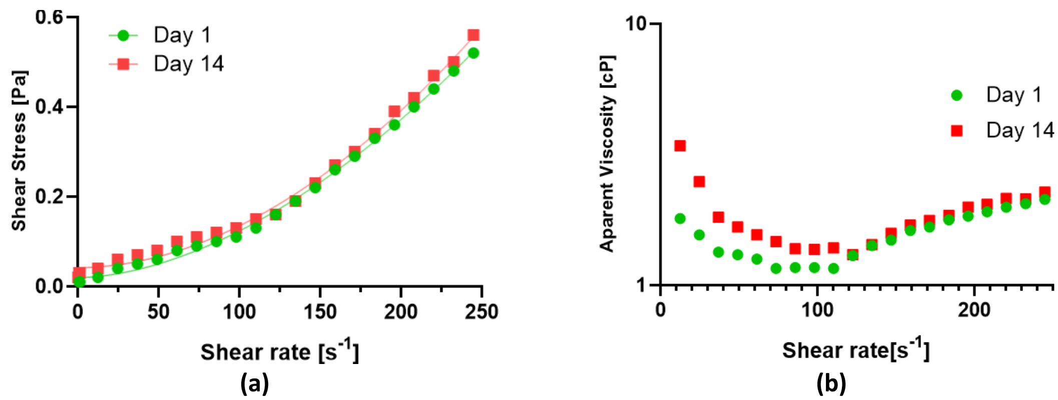

Figure 6. Initial and final rheological monitoring during the bioremediation process: (a) Rheogram (b) Apparent viscosities.

Figure 6b shows the apparent viscosity profiles of the initial and final samples from the microalgae treatment in the airlift photobioreactor. An increasing trend in apparent viscosity was observed in the final sample. It has been demonstrated that a moderate increase in apparent viscosity can be interpreted as a positive indicator of the process, as it evidences active growth, high cell productivity, and possible capture of dissolved organic matter in the liquid phase (Attar *et al*., 2023). This behavior, accompanied by initial, intermediate, and final variations in rheological parameters such as the consistency index (k) and the flow index (n) obtained from correlations with the models, allows the establishment of process control zones where the system is identified as having reached its maximum efficiency in both contaminant removal and biomass production. Similarly, the analysis of these parameters facilitates the determination of critical operating conditions that indicate the appropriate time to perform biomass extraction, thereby avoiding system saturation or losses in treatment efficiency.

The results of the rheological variables according to the commonly used models are shown in Table 2; the flow index n was greater than 1 in all the samples analyzed, therefore they were considered dilatant. In this case, the Herschel-Bulkley model had the correlation coefficient closest to unity, and therefore provided the best fit to the data. An increasing trend in the flow index n was observed during the sampling period, reaching a maximum value of 1.905 on day 14. This suggests that as microalgal biomass accumulates, these structures compact and reorganize under agitation, causing an increase in apparent viscosity at higher deformation rates. This behavior is similar to that reported by Gutiérrez-Casiano *et al*. (2022), who conducted a rheological monitoring of wastewater bioremediation from a poultry processing plant using *Chlorella vulgaris* in an airlift photobioreactor over 16 days. In the three samplings recorded (initial, intermediate, and final), the index n increased during the first 8 days of the process, which was related to the exponential phase of cell growth. In the last sampling, a slightly lower n value was recorded compared to the intermediate value, attributable to the decrease in cell-to-cell interactions and the generation of EPS due to the cell death phase. Therefore, an increase in n can be considered an indirect indicator of the accumulation of active biomass and the structural complexity of the system.

Table 2. Rheological parameters during the biodegradation process

Day	Model	τ_0	K	n	R^2
0	Ostwald de Waele	-	8.517e-005	1.583	0.9937
	Newton	-	0.001792	-	0.9356
	Herschel Bulkley	0.01985	3.186e-005	1.758	0.9974
2	Ostwald de Waele	-	8.831e-005	1.573	0.9918
	Newton	-	0.001754	-	0.9347
	Herschel Bulkley	0.02242	2.845e-005	1.773	0.9968
4	Ostwald de Waele	-	9.607e-005	1.554	0.9933
	Newton	-	0.001729	-	0.9388
	Herschel Bulkley	0.01907	3.725e-005	1.721	0.9970
6	Ostwald de Waele	-	9.657e-005	1.564	0.9884
	Newton	-	0.001834	-	0.9325
	Herschel Bulkley	0.02860	3.047e-005	1.764	0.9963
8	Ostwald de Waele	-	0.0001231	1.517	0.9871
	Newton	-	0.001828	-	0.9385
	Herschel Bulkley	0.02894	2.309e-005	1.818	0.9947
10	Ostwald de Waele	-	0.0002362	1.422	0.9736
	Newton	-	0.002139	-	0.9405
	Herschel Bulkley	0.04577	2.884e-005	1.758	0.9872
12	Ostwald de Waele	-	0.0001213	1.521	0.9817
	Newton	-	0.001839	-	0.9334
	Herschel Bulkley	0.03566	1.961e-005	1.844	0.9938
14	Ostwald de Waele	-	0.0001264	1.520	0.9792
	Newton	-	0.001905	-	0.9313
	Herschel Bulkley	0.04199	1.453e-005	1.905	0.9949

The correlation between the flow index (n) and cell density revealed a logarithmic relationship (equation 7), as shown in Figure 7a, with a determination coefficient of $R^2 = 0.9182$. This strong correlation suggests that the rheological behavior of the treated effluent within the reactor is closely associated with the development and accumulation of microalgal biomass. Specifically, the increase in cell density from 1.7×10^6 to 1.2×10^7 cells/mL resulted in a progressive rise in the flow index from 1.74 to 1.90. The logarithmic fit highlights that the greatest variations in the flow index occur at lower cell densities, whereas at higher concentrations the system tends to stabilize.

In a microalgae-based bioremediation system, a decrease in the consistency index (k) has been demonstrated to be a positive indicator of the removal of colloidal organic matter from wastewater (Schneider and Gerber, 2014). The consistency index remained constant in the range of $3 \times 10^{-5} – 2.3 \times 10^{-5}$ during the first 10 days of the process; however, from day 12 to day 14, it decreased to a value of 1.453×10^{-5}. These values can be related to the results obtained from the decrease in COD, since between days 2 and 10 the values fluctuated between 500 mg/L and 400 mg/L, until days 12 and 14, when a downward trend was observed. The behavior of this correlation is shown in Figure 7b, where the relationship between the consistency index (K) and the COD_s concentration exhibited a logarithmic fit (Equation 8) with a correlation coefficient of $R^2 = 0.8144$, indicating a consistent association between both variables. Nevertheless, the R^2 value lower than 0.9 suggests that the relationship is not fully explained by soluble COD concentration alone. This can be attributed to the fact that organic matter comprises both biodegradable and non-biodegradable compounds, the latter being metabolically unavailable but potentially contributing indirectly to the fluid viscosity. At the beginning of the process, the microalgal biomass primarily consumes biodegradable organic compounds; however, as the process progresses, the degradation rate decreases due to the predominance of non-biodegradable organic matter and only a minor fraction of biodegradable compounds.

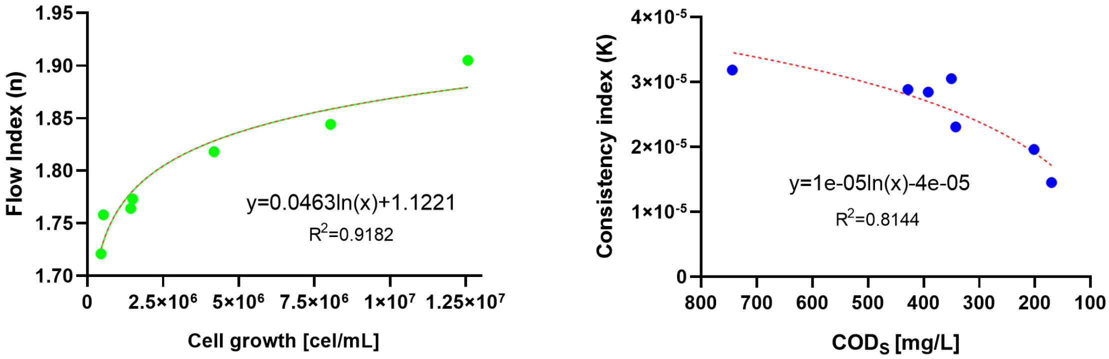

$$y = 0.0463\, ln\,(x) + 1.1221 \qquad (7)$$

$$y = 1e - 05\, ln\,(x) - 4e - 05 \qquad (8)$$

(a) **(b)**

Figure 7. Correlation of (a) Flow index with cell density (b) Consistency index with CODs.

Conclusions

The MWW proved to be a suitable medium for the growth of *H. pluvialis*. Furthermore, adaptation tests showed that at low inoculum concentrations, inhibition phenomena caused by high substrate competition and self-shading are avoided. On the other hand, in the 400 mL photobioreactor experiments for the 3 inoculum levels evaluated, the organic matter content was effectively reduced, achieving removals greater than 64% of total COD and 92% of COD_S.

During the scale-up in the airlift photobioreactor, removals close to 80% of COD_S were obtained, and effective consumption of N and P was achieved, with both parameters remaining below the maximum permissible ranges according to Mexican regulations (NOM-001-SEMARNAT-2021). This confirms that the implementation of the airlift photobioreactor with the proposed configuration favored the optimal development of the culture, increasing the efficiency of pollutant removal and cell productivity.

The rheological monitoring carried out simultaneously with the kinetics of pollutant removal showed a dilatant behavior (n>1) characteristic of systems that use microalgae, and the affinity for fitting with the Herschel-Bulkley model allowed for establishing relationships of change with the rheological parameters of consistency index (k) and flow index (n). Monitoring these variables offers an indirect but robust approach to evaluate the physiological state of the culture, biomass accumulation, and the efficiency of soluble organic matter removal, which makes rheology a strategic control tool for the wastewater treatment process with the microalga *H. Pluvialis*.

Acknowledgments and Funding: The financial support granted by CONACYT through the scholarship with CVU 1323199.

Author contributions: U.C.-R.: writing, data collection, analysis and interpretation of data; J.M.M.-C.: editing, supervision, project administration and analysis of data; R.E.S.-P., J.E.-G., A.A.-L. and E.H.-A.: editing, conceptualization and data analysis.

References

Abdel-Raouf, N., Al-Homaidan, A., & Ibraheem, I. (2012). Microalgae and wastewater treatment. *Saudi Journal of Biological Sciences*, *19*(3), 257–275. https://doi.org/10.1016/j.sjbs.2012.04.005

Adesanya, V. O., Vadillo, D. C., & Mackley, M. R. (2012). The rheological characterization of algae suspensions for the production of biofuels. *Journal of Rheology*, *56*(4), 925–939. https://doi.org/10.1122/1.4717494

Amaro, H. M., Salgado, E. M., Nunes, O. C., Pires, J. C., & Esteves, A. F. (2023). Microalgae systems - environmental agents for wastewater treatment and further potential biomass valorisation. *Journal of Environmental Management*, *337*, 117678. https://doi.org/10.1016/j.jenvman.2023.117678

APHA, Wpcf, & AWWA. (2017). Standard methods for the examination of water and wastewater (23rd ed.). APHA.

Ata, R., Tore, G. Y., & Shah, M. P. (2021). Emerging technologies for treatment of antibiotic residues from wastewater influent/effluent for sustainable environment: A case study with NFC-doped titania immobilized on polystyrene as an efficient technology. *Current Research in Green and Sustainable Chemistry*, *4*, 100065. https://doi.org/10.1016/j.crgsc.2021.100065

Attar, S. B., Morillas-España, A., Sánchez-Zurano, A., Pessôa, L. C., Pinna-Hernández, M. G., De Jesus Assis, D., López, J. L. C., & Acién, G. (2023b). Influence of culture media composition on the rheology of microalgae concentrates on a large scale. New Biotechnology, 77, 90–99. https://doi.org/10.1016/j.nbt.2023.07.005

Azam, H. M., & Finneran, K. T. (2013). Fe(III) reduction-mediated phosphate removal as vivianite (Fe3(PO4)2·8H2O) in septic system wastewater. *Chemosphere*, *97*, 1–9. https://doi.org/10.1016/j.chemosphere.2013.09.032

Behin, J., & Amiri, P. (2023). A review of recent advances in airlift reactors technology with emphasis on environmental remediation. *Journal of Environmental Management*, *335*, 117560. https://doi.org/10.1016/j.jenvman.2023.117560

Bio6. (n.d.). https://rmiq.org/iqfvp/Pdfs/Vol.%2015,%20No.%202/Bio6/eBio6.html

Benner, P., Meier, L., Pfeffer, A., Krüger, K., Vargas, J. E. O., & Weuster-Botz, D. (2022). Lab-scale photobioreactor systems: principles, applications, and scalability. *Bioprocess and Biosystems Engineering*, *45*(5), 791–813. https://doi.org/10.1007/s00449-022-02711-1

De Moraes, L. B. S., Mota, G. C. P., Santos, E. P. D., Da Silva Campos, C. V. F., Da Silva, B. a. B., Gálvez, A. O., & De Souza Bezerra, R. (2023). Haematococcus pluvialis cultivation and astaxanthin production using different nitrogen sources with pulse feeding strategy. *Biomass Conversion and Biorefinery*, *14*(14), 16231–16243. https://doi.org/10.1007/s13399-023-03824-7

Estrada-García, J., Hernández-Aguilar, E., Romero-Mota, D. I., & Méndez-Contreras, J. M. (2023). Influence of anaerobic biotransformation process of agro-industrial waste with Lactobacillus acidophilus on the rheological parameters: case of study of pig manure. *Archives of Microbiology*, *205*(3). https://doi.org/10.1007/s00203-023-03437-8

Fu, J., Huang, Y., Liao, Q., Xia, A., Fu, Q., & Zhu, X. (2019). Photo-bioreactor design for microalgae: A review from the aspect of CO2 transfer and conversion. *Bioresource Technology*, *292*, 121947. https://doi.org/10.1016/j.biortech.2019.121947

Gutiérrez-Casiano, N., Hernández-Aguilar, E., Alvarado-Lassman, A., & Méndez-Contreras, J. M. (2022). Removal of carbon and nitrogen in wastewater from a poultry processing plant in a photobioreactor cultivated with the microalga Chlorella vulgaris. *Journal of Environmental Science and Health Part A*, *57*(7), 620–633. https://doi.org/10.1080/10934529.2022.2096986

Gutiérrez-Casiano, N., Hernández-Aguilar, E., Alvarado-Lassman, A., & Méndez-Contreras, J. M. (2022). Removal of carbon and nitrogen in wastewater from a poultry processing plant in a photobioreactor cultivated with the microalga Chlorella vulgaris. *Journal of Environmental Science and Health Part A*, *57*(7), 620–633. https://doi.org/10.1080/10934529.2022.2096986

Han, W., Jin, W., Li, Z., Wei, Y., He, Z., Chen, C., Qin, C., Chen, Y., Tu, R., & Zhou, X. (2021). Cultivation of microalgae for lipid production using municipal wastewater. *Process Safety and Environmental Protection*, *155*, 155–165. https://doi.org/10.1016/j.psep.2021.09.014 Huang, Y., Ragush, C. M., Johnston, L. H., Hall, M. W., Beiko, R. G., Jamieson, R. C., & Hansen, L. T. (2021). Changes in bacterial communities during treatment of municipal wastewater in arctic wastewater stabilization ponds. Frontiers in Water, 3. https://doi.org/10.3389/frwa.2021.710853

Jeong, D., & Jang, A. (2021). Mitigation of self-shading effect in embedded optical fiber in Chlorella sorokiniana immobilized polyvinyl alcohol gel beads. *Chemosphere*, *283*, 131195. https://doi.org/10.1016/j.chemosphere.2021.131195

Khalid, A. a. H., Yaakob, Z., Abdullah, S. R. S., & Takriff, M. S. (2018). Analysis of the elemental composition and uptake mechanism of Chlorella sorokiniana for nutrient removal in agricultural wastewater under optimized response surface methodology (RSM) conditions. *Journal of Cleaner Production*, *210*, 673–686. https://doi.org/10.1016/j.jclepro.2018.11.095

Laroche, C. (2022). Exopolysaccharides from Microalgae and Cyanobacteria: Diversity of Strains, Production Strategies, and Applications. *Marine Drugs*, *20*(5), 336. https://doi.org/10.3390/md20050336

Li, L., Xu, X., Wang, W., Lau, R., & Wang, C. (2022). Hydrodynamics and mass transfer of concentric-tube internal loop airlift reactors: A review. *Bioresource Technology*, *359*, 127451. https://doi.org/10.1016/j.biortech.2022.127451

Mathew, M. M., Khatana, K., Vats, V., Dhanker, R., Kumar, R., Dahms, H., & Hwang, J. (2022). Biological Approaches Integrating Algae and Bacteria for the Degradation of Wastewater Contaminants—A Review. *Frontiers in Microbiology*, *12*. https://doi.org/10.3389/fmicb.2021.801051

Mazziero, V. T., Batista, V. G., De Oliveira, D. G., Scontri, M., De Paula, A. V., & Cerri, M. O. (2022). Characterization of packed-bed in the downcomer of a concentric internal-loop airlift bioreactor. *Biochemical Engineering Journal*, *181*, 108407. https://doi.org/10.1016/j.bej.2022.108407

Nahidian, B., Ghanati, F., Shahbazi, M., & Soltani, N. (2018). Effect of nutrients on the growth and physiological features of newly isolated Haematococcus pluvialis TMU1. *Bioresource Technology*, *255*, 229–237. https://doi.org/10.1016/j.biortech.2018.01.130

Onyeaka, H., Miri, T., Obileke, K., Hart, A., Anumudu, C., & Al-Sharify, Z. T. (2021). Minimizing carbon footprint via microalgae as a biological capture. *Carbon Capture Science & Technology*, *1*, 100007. https://doi.org/10.1016/j.ccst.2021.100007

Pan, M., Zhu, X., Pan, G., & Angelidak, I. (2021). Integrated valorization system for simultaneous high strength organic wastewater treatment and astaxanthin production from Haematococcus pluvialis. *Bioresource Technology*, *326*, 124761. https://doi.org/10.1016/j.biortech.2021.124761

Pérez-Guzmán, S. M., Hernández-Aguilar, E., Rosas-Mendoza, E. S., Alvarado-Lassman, A., & Méndez-Contreras, J. M. (2024). Efecto de la presión de saturación en la operación en modo batch de un reactor DAF escala laboratorio para el tratamiento de efluentes municipales. *Tendencias en Energías Renovables y Sustentabilidad* ., *3*(1), 139–144. https://doi.org/10.56845/terys.v3i1.218

Płuciennik-Koropczuk, E., & Myszograj, S. (2019). New approach in COD fractionation methods. *Water*, *11*(7), 1484. https://doi.org/10.3390/w11071484

Qiu, R., Gao, S., Lopez, P. A., & Ogden, K. L. (2017). Effects of pH on cell growth, lipid production and CO2 addition of microalgae Chlorella sorokiniana. *Algal Research*, *28*, 192–199. https://doi.org/10.1016/j.algal.2017.11.004

Radice, R. P., Grassi, G., Capasso, G., Montagnuolo, E., Aiello, D., Perna, A. M., Marzocco, S., & Martelli, G. (2024). Five mutated genotypes of Haematococcus pluvialis useful for crude oil wastewater bioremediation. *Algal Research*, *83*, 103693. https://doi.org/10.1016/j.algal.2024.103693

Robles-Heredia, J. C., Sacramento-Rivero, J. C., Ruiz-Marín, A., Baz-Rodríguez, S., Canedo-López, Y., & Narváez-García, A. (2016). Evaluation of cell growth, nitrogen removal and lipid production by chlorella vulgaris to different conditions of aeration in two types of annular photobioreactors. *Revista Mexicana De Ingeniería Química*, *15*(2), 361–377.

Rout, P. R., Shahid, M. K., Dash, R. R., Bhunia, P., Liu, D., Varjani, S., Zhang, T. C., & Surampalli, R. Y. (2021). Nutrient removal from domestic wastewater: A comprehensive review on conventional and advanced technologies. *Journal of Environmental Management*, *296*, 113246. https://doi.org/10.1016/j.jenvman.2021.113246

Sales-Pérez, R. E., Sales-Chávez, R. M., Romero-Mota, D. I., Estrada-García, J., & Méndez-Contreras, J. M. (2023a). Removal of organic matter during adaptation of Nannochloropsis oculata in livestock waste. *Renewable Energy Biomass & Sustainability*, *5*(2), 32–39. https://doi.org/10.56845/rebs.v5i2.93

Schneider, N., & Gerber, M. (2014). Correlation between viscosity, temperature and total solid content of algal biomass. *Bioresource Technology*, 170, 293–302. https://doi.org/10.1016/j.biortech.2014.07.107

Simha, P., Vasiljev, A., Randall, D. G., & Vinnerås, B. (2023). Factors influencing the recovery of organic nitrogen from fresh human urine dosed with organic/inorganic acids and concentrated by evaporation in ambient conditions. *The Science of the Total Environment*, *879*, 163053. https://doi.org/10.1016/j.scitotenv.2023.163053

Singh, V., Phuleria, H. C., & Chandel, M. K. (2017). Greenhouse Gas Emissions from Sewage Treatment Plants Based on Sequential Batch Reactor in Maharashtra. In Water science and technology library. In V. Singh, S. Yadav, & R. Yadava (Eds.), *Climate change impacts* (pp. 195–210). Springer.https://doi.org/10.1007/978-981-10-5714-4_13

Sobolewska, E., Borowski, S., & Nowicka-Krawczyk, P. (2024). Cultivation of microalgae in liquid digestate to remove nutrients and organic contaminants. *BioEnergy Research*, *17*(3), 1843–1855. https://doi.org/10.1007/s12155-024-10753-4

Su, Y. (2020). Revisiting carbon, nitrogen, and phosphorus metabolisms in microalgae for wastewater treatment. *The Science of the Total Environment*, *762*, 144590. https://doi.org/10.1016/j.scitotenv.2020.144590

Tang, J., Qu, X., Chen, S., Pu, Y., He, X., Zhou, Z., Wang, H., Jin, N., Huang, J., Shah, F., Hu, Y., & Abomohra, A. (2023). Microalgae cultivation using municipal wastewater and anaerobic membrane effluent: lipid production and nutrient removal. *Water*, *15*(13), 2388. https://doi.org/10.3390/w15132388

Uyar, B., Ali, M. D., & Uyar, G. E. O. (2024). Design parameters comparison of bubble column, airlift and stirred tank photobioreactors for microalgae production. *Bioprocess and Biosystems Engineering*, *47*(2), 195–209. https://doi.org/10.1007/s00449-023-02952-8

Vega, J. M. (2018). Nitrogen and sulfur metabolism in microalgae and plants: 50 years of research. In F. Cánovas, U. Lüttge, C. Leuschner, & M. C. Risueño (Eds.), *Progress in botany* (Vol. 81, pp. 143–169). Springer. https://doi.org/10.1007/124_2018_26

Wang, H., Qi, B., Jiang, X., Jiang, Y., Yang, H., Xiao, Y., Jiang, N., Deng, L., & Wang, W. (2019). Microalgal interstrains differences in algal-bacterial biofloc formation during liquid digestate treatment. *Bioresource Technology*, *289*, 121741. https://doi.org/10.1016/j.biortech.2019.121741

Whitton, R., Ometto, F., Pidou, M., Jarvis, P., Villa, R., & Jefferson, B. (2015). Microalgae for municipal wastewater nutrient remediation: mechanisms, reactors and outlook for tertiary treatment. *Environmental Technology Reviews*, *4*(1), 133–148. https://doi.org/10.1080/21622515.2015.1105308

Wu, Z., Duan, H., Li, K., & Ye, L. (2022). A comprehensive carbon footprint analysis of different wastewater treatment plant configurations. *Environmental Research*, *214*, 113818. https://doi.org/10.1016/j.envres.2022.113818

Xu, H., Tang, Z., Yang, D., Dai, X., & Chen, H. (2023). Enhanced growth and auto-flocculation of Scenedesmus quadricauda in anaerobic digestate using high light intensity and nanosilica: A biomineralization-inspired strategy. *Water Research*, *235*, 119893. https://doi.org/10.1016/j.watres.2023.119893

Xu, L., Weathers, P. J., Xiong, X., & Liu, C. (2009). Microalgal bioreactors: Challenges and opportunities. *Engineering in Life Sciences*, *9*(3), 178–189. https://doi.org/10.1002/elsc.200800111

Zhang, W., Yong, Y., Zhang, G., Yang, C., & Mao, Z. (2014). Mixing Characteristics and Bubble Behavior in an Airlift Internal Loop Reactor with Low Aspect Ratio. *Chinese Journal of Chemical Engineering*, *22*(6), 611–621. https://doi.org/10.1016/s1004-9541(14)60089-6

Zhou, J., Yang, L., Huang, K., Chen, D., & Gao, F. (2022). Mechanisms and application of microalgae on removing emerging contaminants from wastewater: A review. *Bioresource Technology*, *364*, 128049. https://doi.org/10.1016/j.biortech.2022.128049